

Top-Down Characterization of Low Voltage Electric Power Distribution Networks for Use of PLC Systems

Antonio A. M. Picorone, Thiago R. Oliveira, Raimundo Sampaio-Neto, *Senior Member, IEEE*,
and Moises V. Ribeiro, *Senior Member, IEEE*

Abstract—This paper presents unprecedented results of a comprehensive measurement campaign based on sounding approach with the aim of characterizing and modeling the outdoor Brazilian as a means of data communication. Average channel attenuation, root-mean-square delay spread, coherence time, coherence bandwidth and achievable data rate are analyzed in the frequency band from 1.7 MHz up to 100 MHz. Statistical models for some channel features are proposed. The cyclically periodic variation of the channel is quantified and presented as a temporal function of the average channel attenuation variation. Also, mathematical models based on only two parameters representing both the background and impulsive noises are proposed. The parameters analyzed in this contribution can help the characterization of outdoor Brazilian power line channels, since increase the knowledge about such communication media, contributing to the design of increasingly robust and efficient PLC systems.

Keywords—power line communication, channel estimation, statistical modeling, channel features.

I. INTRODUCTION

THE development of data communication systems capable of interconnecting the most diverse electro-electronic devices has motivated many researchers lately. Smart cities [1], smart buildings [2] and smart grids [3] are examples that can only be realized through a communication network that integrates existing technologies in homes, in vehicles, in commerce, in the electric power network, etc. Furthermore, much of this integration has been discussed within concept of Internet of Things (IoT) [4]. On the other hand, nowadays there is no single technology that meets all requirements necessary for the interconnection of the present devices, given the diversity and complexity of the environments to be integrated. Consequently, there are combinations of a wide variety of communication systems that are used for this purpose [5], [6].

When smart grids are considered, power line communication (PLC) emerges as a natural choice largely evaluated in the

literature [7]–[9]. One of the great motivations of the use of this technology lies in the infrastructure that has already been installed and its great potential for network convergence [6], [10], [11]. Though PLC is potentially convenient for low-cost data transmission for measurement and control of electricity supply, water and gas consumption, and in industries, the electric power grids constitute a challenging medium for data communication since they were not designed for this purpose [12]–[14]. In order to design an efficient communication system, regardless the type of system, the knowledge of the effects that a communication signal is subjected through its propagation in the communication medium is mandatory. This effects are usually evaluated as a function of some channel parameters, such as average channel attenuation (ACA), root-mean-square delay spread (RMS-DS), coherence bandwidth (CB), and coherence time (CT).

The propagation characteristics of PLC signals in indoor low voltage networks are well-known in the literature [15]–[18], due mainly to the ease physical access to the networks. On the other hand, although knowledge of medium characteristics is extremely important, papers with a focus on low voltage power distribution network (LV-PDN) are not common in the literature, due mainly to the complexity of conducting measurement campaigns in these environments. In [19] a measurement campaign was carried out in Germany. In that work, the ACA, noise, and RMS-DS of the PLC outdoor channels (LV-PDN) in the 1 MHz up to 30 MHz frequency band were evaluated. The results of a small measurement campaign was presented in [20] and aimed to characterize the LV-PDN for outdoor PLC communication in India. The results reported in [20] are also restricted to the frequency band from 1 MHz up to 30 MHz and evaluated the ACA, RMS-DS and CB. For outdoor PLC channels, [19] reported values of $1.4 \mu\text{s}$ considering a single frequency of 3.75 MHz and of $0.8 \mu\text{s}$ for the 5 MHz frequency. However, it has not been clearly defined whether these values represent channel impulse response (CIR) duration or the RMS-DS value. Values of RMS-DS between $0.145 \mu\text{s}$ and $0.228 \mu\text{s}$ in the frequency range of 1.7 MHz up to 30 MHz were reported by [20].

In general, the behavior of LV-PDN when used as a data communication medium is not yet well-known. In order to contribute to mitigate this gap, this work aims to increase the scientific knowledge about the characteristics of LV-PDV as a means of data communication. Towards this end, the main contributions of this paper are summarized as follows:

A. A. M. Picorone (antonio.picorone@ufjf.edu.br) is with the Production Engineering and Mechanics Department, Federal University of Juiz de Fora (UFJF), Juiz de Fora, Brazil.

T. R. Oliveira (thiago.oliveira@ifsudestemg.edu.br) is with the Electronics Department, Federal Institute of Education, Science and Technology of the Southeast of Minas Gerais (IFSEMG), Campus Juiz de Fora, Brazil.

R. Sampaio-Neto (raimundo@cetuc.puc-rj.br) is with the Pontifícia Universidade Católica do Rio de Janeiro (PUC-RJ), Rio de Janeiro, Brazil.

M. V. Ribeiro (mrbeiro@ieee.org) is with the Electrical Engineering Department, Federal University of Juiz de Fora (UFJF), and Smarti9 Ltda, Brazil.

- Results of an extensive measurement campaign conducted in the outdoor Brazilian LV-PDN are presented with the objective of helping to characterize these networks as a means of PLC communication. The measurement campaign was carried out during 14 days in two distinct districts of the city of Juiz de Fora, MG, Brazil;
- Results are presented of numerical analyzes performed on the data obtained from the measurement campaign that help the characterization of LV-PDN as a PLC communication medium. The analyzed channel features are ACA, RMS-DS, CB, CT, and achievable data rate (ADR);
- The background and impulsive noises observed in the measurement campaign of outdoor Brazilian LV-PDN are analyzed and presented.

Based on numerical analyses, we state the following remarks:

- It was observed and quantified the time window occupied by the abrupt ACA variation due to the cyclic switching of charges synchronized with the electric power network. Statistically, RMS-DS presents values following, with good approximation, the inverse Gaussian probability distribution;
- The CB presents values following, with good approximation, a inverse Gaussian probability distribution;
- Only in 20% of the analyzed cases the CT was less than, approximately, 2 ms for $\beta = 0.99$ and 5 ms for $\beta = 0.95$. The CT was not lower than 1.38 ms and 5.76 ms, for $\beta = 0.99$ and $\beta = 0.90$, respectively.

The rest of paper is organized as follows: Section II the measurement setup and campaign are presented. Section III parameters used to channel characterize are defined. The results of measurement campaign are presented in the Section IV. Finally, the conclusions of this study are presented in Section V.

II. MEASUREMENT SETUP AND CAMPAIGN

The statistical characterization and modeling of the features associated with Brazilian outdoor PLC channels were supported by estimates of channel frequency response (CFR). The data used to estimate the CFR were produced by a set of measurement equipment during a measurement campaign in the city of Juiz de Fora, MG, Brazil, as discussed bellow.

A. Measurement Setup

The block diagram of the adopted measurement setup applied in order to estimate the CFR is depicted in Fig. 1 and consists of three main components:

- (i) Signal generator: Device composed of an arbitrary signal generator board mounted in a rugged computer. A pre-designed sounding sequence is loaded into it and converted to an analog signal to be submitted to the electric power grid under analysis;
- (ii) Data digitizer: Acts as a receiver, measuring the transmitted sounding signal after propagating through the electric power grid, and converts it into a digital representation

- (iii) Coupler: Circuitry applied to connect both the signal generator and data digitizer to the electric power grid under analysis. The coupler is essentially composed of an analog high pass filter, blocking the main voltage signal (60 Hz in Brazil) that can damage the other equipments [21]. Insertion loss lower than 2 dB in the frequency band between 1.7 MHz up to 100 MHz is introduced by adopted coupler.

The set of equipment and algorithms used to inject the test signal into the LV-PDN is called Setup TX. On the other hand, the set of equipment and algorithms used to sample and estimate the LV-PDN CFR is denominated Setup RX.

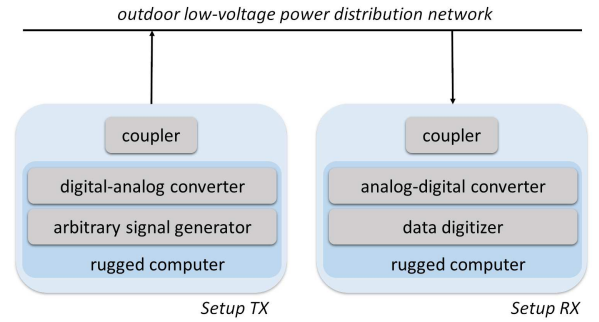


Fig. 1: Block diagram of the measurement setup.

The CFR estimates were obtained through the estimation methodology described in [22], which is based on a sounding approach [23]. The set of adopted parameters in the estimation methodology is summarized in Tab. I. Essentially, the transmitted signal is composed of Hermitian symmetric orthogonal frequency division multiplexing (HS-OFDM) symbols [24]. By adopting 200 MHz sampling frequency, the frequency resolution is around 48.83 kHz and each CFR estimate is obtained every 23.04 μ s, approximately – for more details see [25].

B. Measurement Campaign

For the analysis of the features of the outdoor PLC channel, 33 cycles of the LV-PDN fundamental frequency (60 Hz in Brazil) were considered at distinct points in a low-income neighborhood of the city of Juiz de Fora, MG, Brazil. The distance between the couplers ranged from 3 m up to 100 m, with mean values of 15 m, 50 m and 85 m. In each cycle of the LV-PDN (16.67 ms), approximately 723 PLC channel frequency responses were collected with a length of 4,096 samples per CFR, in addition to the cyclic prefix of size equal to 512. With this, 23,919 CFR measurements of outdoor PLC channels were evaluated in total.

The measurement of the noise in the outdoor PLC channel was performed according to [26], in which groups of 3,500,000 successive samples of voltage in the time domain of the signal on the LV-PDN were obtained in the absence of signal emitted

by the signal generator. Each sample group corresponds to approximately 17.5 ms. This time was chosen based on the memory capacity of the data acquisition board when set to a sampling rate of 200 Msps. These samples were acquired in one of the three phases of the LV-PDN and form the database of outdoor PLC channel noise.

TABLE I: Main parameters adopted for the CFR estimation.

Description	Value
Sampling frequency	$f_s = 200$ MHz
Number of sub-carriers	$N = 2,048$
Modulation	BPSK
Cyclic prefix length	$L_{cp} = 512$
Frequency resolution	$\Delta_f = 48.83$ kHz
Symbol duration	$23.04 \mu s$
Length of the sequence $\{y_j[n]\}$	$L_j = 9,216$
Number of samples used to compute \mathbf{m}_t	$K_d = 8$
Number of shift in the vector \mathbf{m}_t calculus	$R = 128$

Figs. 2 and 3 illustrate the complex task of installing the setups used as transmitter and receiver in a part of the measurement campaign.



Fig. 2: Setup RX installed on the LV-PDN pole.

III. FEATURES DEFINITIONS

Let us assume the PLC channels are modeled as band limited and frequency selective wide-sense stationary uncorrelated scattering (WSSUS). Also, assume that during a certain period of time, the CIR is time-invariant. Therefore, the CIR of the PLC channel is during this certain time interval is $h(t) \in \mathbb{R}|t \in [0, T_h)$, and its corresponding Fourier transform is $H(f) \in \mathbb{C}|f| < B$, in which B is the frequency bandwidth. Note that $h[n] = h(t)|_{t=nT_s}$, in which $n = 0, 1, 2, \dots, L_h - 1$ and T_s is the sampling period. The features extracted from the Brazilian PLC channels are described in the following subsections. This assumption is taken into account to define ACA, average channel frequency response (ACFR), RMS-DS, CT and CB.



Fig. 3: Setup TX installed near the consumer's electric power meter.

A. Average Channel Attenuation

The ACA in dB is expressed by

$$ACA = -10 \log_{10} \left(\frac{1}{N} \sum_{k=0}^{N-1} |H[k]|^2 \right) \quad [\text{dB}], \quad (1)$$

where $H[k]$ is the k^{th} coefficient of the discrete channel frequency response for the zero-padded version of the discrete-time impulse response of the time invariant PLC channel $\{h[n]\}_{n=0}^{L_h-1}$ because $L_h \ll N$.

B. Average Channel Frequency Response

The ACFR represents the mean of all measured CFR in the measurement campaign carried out, it is expressed by

$$\bar{A}_f = 20 \log_{10} [E\{|H[k]|\}] \quad [\text{dB}], \quad (2)$$

where $E\{\cdot\}$ denotes the expectation operator.

C. Root Mean Squared Delay Spread

The RMS-DS represents the distribution of the transmitted power over various paths in a multipath environment, and can be defined as the square root of the second central moment of a power delay profile. For a discrete-time channel impulse response, the RMS-DS (σ_τ) is expressed as

$$\sigma_\tau = T_s \sigma_0 = T_s \sqrt{\mu'_0 - \mu_0^2}, \quad (3)$$

where

$$\mu_0 = \frac{\sum_{n=0}^{L_h-1} n |h[n]|^2}{\sum_{n=0}^{L_h-1} |h[n]|^2} \quad \text{and} \quad \mu'_0 = \frac{\sum_{n=0}^{L_h-1} n^2 |h[n]|^2}{\sum_{n=0}^{L_h-1} |h[n]|^2}, \quad (4)$$

and $T_s = 1/f_s$ is the sampling period. Note that σ_0 is the RMS-DS normalized to a unitary sampling time, μ_0 is the

average delay and $h[n]$ is the n^{th} sample of the discrete-time channel impulse response. The channel impulse response is evaluated over the support of the channel impulse response in the discrete-time domain.

D. Coherence Bandwidth

The coherence bandwidth reflects how selective the channel frequency response is, being determined by

$$R(e^{j\omega}) = \int_{-\pi}^{\pi} H(e^{j\omega}) H^*(e^{j\omega+\Delta\omega}) d\omega, \quad (5)$$

in which $H(e^{j\omega})$ is the Fourier transform of the discrete-time representation of a linear and time invariant PLC channel and $0 \leq \Delta\omega \leq 2\pi$ denotes the angular frequency resolution in the transform domain. The value of the coherence bandwidth ($\Delta\omega_{B_c}$) in the discrete-time domain is such that

$$|R(e^{j\Delta\omega_{B_c}})| = \gamma |R(1)|, \quad (6)$$

where $0 < \gamma < 1$ is the correlation level informing that the channel frequency response does not vary considerably when $\Delta\omega \in [0, \Delta\omega_{B_c}]$. Assuming a sampling frequency equal to $f_s = 2B$ Hz, in which B is the frequency bandwidth, then the coherence bandwidth (B_c) is expressed as

$$B_c = \frac{\Delta\omega_{B_c}}{2\pi} f_s. \quad (7)$$

The CB estimates from the measured PLC channels are analyzed with respect to the correlation coefficient $\gamma = 0.9$.

E. Coherence Time

The coherence time is the time duration in which the channel impulse response of a PLC channel is considered time invariant. Following [27], the evaluation of the coherence time may be carried out by assuming that the PLC channel is an WSSUS process. Then, the coherence time of the channel is related to the coherence time of the complex gains of the channel, $\alpha_l(t)$, which incorporate both attenuation and phase deviations due to $l = 1, 2, \dots, L$ multiple reflections of the signal in the communication medium.

In its turn, the coherence index between samples of $\alpha_l(t)$, taken Δt time units apart, is given by

$$\rho_{\alpha_l} = \frac{E[\alpha_l(t) \alpha_l^*(t + \Delta t)]}{E[|\alpha_l(t)|^2]}, \quad (8)$$

in which $E[\cdot]$ is the expectation operator and $*$ denotes the conjugate operator. Thus, it can be assumed that the correlation index of the PLC channel is given by

$$\rho_h(\Delta t) = \frac{\sum_{l=1}^L P_l \rho_{\alpha_l}(\Delta t)}{\sum_{l=1}^L P_l}; \quad 0 \leq |\rho_h(\Delta t)| \leq 1, \quad (9)$$

where $P_l = E[|\alpha_l(t)|^2]$ is the average power of the l^{th} path. Hence, the CT of the channel can be obtained through

$$|\rho_h(T_c^\beta)| \geq \beta, \quad (10)$$

where $0 < \beta < 1$ refers to the minimum correlation index admitted to characterize the channel as time-invariant during the time interval $\Delta t = T_c^\beta$. By adopting an hermitian symmetric orthogonal frequency division multiplexing (HS-OFDM) scheme, which is the version of the orthogonal frequency division multiplexing (OFDM) scheme for baseband data communication [24], the CT for the correlation index β , denoted by T_c^β , can be estimated by using [27]

$$T_c^\beta = M_c(2N + L_{cp})T_s, \quad (11)$$

where M_c is the number of consecutive channel estimates that is needed to reach a correlation equal to $0 < \beta < 1$, where $T_s = 1/f_s$ denotes the sampling period, $2N$ is the number of subcarriers and L_{cp} is the length of the cyclic prefix in the HS-OFDM symbol.

F. Achievable Data Rate

Let us assume that the PLC channel being frequency selective, the additive noise being colored Gaussian random process, N ensures that the subchannels as flat and the power spectral densities (PSD) of the additive noise flat, then the achievable data rate can be obtained by using [28]

$$R = \max_{S_x[k]} \frac{B}{N} \sum_{k=0}^{N-1} \log_2 \left(1 + \frac{S_x[k] |H[k]|^2}{S_n[k]} \right) \quad [\text{bps}], \quad (12)$$

subject to $\sum_{k=0}^{N-1} B S_x[k] \leq P_x$. Note that $S_x[k]$ and $S_n[k]$ denote the PSD of the transmitted signal at the k^{th} subcarrier and the PSD of the additive noise in the k^{th} subchannel. Also, P_x is the total transmission power.

IV. RESULTS

This paper presents some important discussions about key parameters estimated from measured Brazilian outdoor PLC channels. These channel parameters are ACA, ACFR, time duration of impulsive response, RMS-DS, CB, CT and achievable data rate. The analyzes were performed considering the distance between the measurement equipments (Setup TX end Setup RX) ranging from 3 m up to 100 m, with average distances of 15 m, 50 m and 85 m and encompasses the frequency band ranging from 1.7 MHz up to 100 MHz.

Some data sets presented (RMS-DS and CB) are modeled by a statistical distribution in which case some continuous distributions are considered, including both symmetric (Logistic, Normal and t-Student) and asymmetric (Exponential, Gamma, Inverse Gaussian, Log-logistic, Log-normal, Nakagami, Rayleigh, Rician and Weibull) distributions. Adherence tests are conducted by evaluating the associated log-likelihood values, which is the adopted metric to support the choice of the best statistical distribution that models such channel parameter.

A. Average Channel Attenuation

The relation between ACA and the channel length can be observed in Fig. 4. As expected, the channel attenuation increases as the channel length increases, with a linear ratio of 0.4 dB/m for the measured Brazilian outdoor PLC channels.

A robust linear approach of the ACA (Model in Fig. 4) based on the mean square error criterion can be given by

$$\tilde{A}_c(d) = 0.4d + 16.71 \text{ [dB]}, \quad (13)$$

where \tilde{A}_c indicates the ACA that the PLC signal will suffer and d is the distance (in meters) between transmitter and receiver.

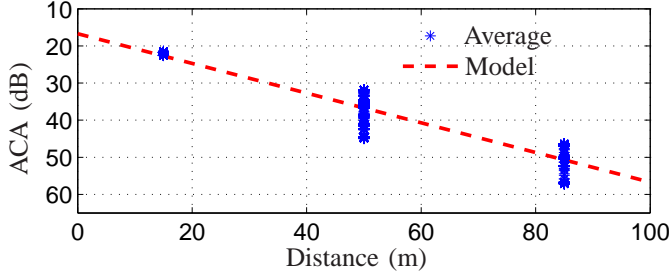


Fig. 4: Average channel attenuation depending on the distance between the transmitter and receiver of PLC signals.

Fig. 5 illustrates the variation of ACA value of one PLC outdoor channel. By comparing with the main signal magnitude (60 Hz in Brazil), these variations in ACA amplitude occurs in a time window centered at the instant time in which the LV-PDN main signal crosses the zero. The observed average duration of the time window occupied by the abrupt ACA variation of measured outdoor PLC channels was $T_{W120} = 0.98$ ms, since the observed values ranged from 0.73 ms up to 1.40 ms. This ACA alteration is related to the switching synchronized with the fundamental frequency of the loads connected to the electric power network. This abrupt and cyclic change in the ACA has been reported in other papers for indoor PLC channels [11], [12].

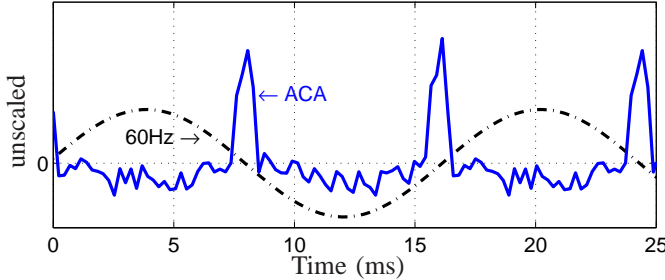


Fig. 5: Temporal window containing the abrupt change of the ACA of the channel PLC outdoor due to zero crossing of the fundamental frequency of LV-PDN

B. Average Channel Frequency Response

The magnitude response of measured PLC channels, in terms of maximum, mean and minimum value, is depicted in Fig. 6. As can be seen, the mean value of the magnitude response of outdoor PLC channels exhibit a decay rate of, approximately, 0.4 dB/MHz. Furthermore, high attenuation

is observed at the initial portion of the analyzed spectrum up to 1.7 MHz due to the action of the high-pass filter of the PLC coupler applied in the measurements. Fig. 6 also shows a robust approach of the mean measured PLC channel attenuation response based on the mean square error criterion, given by

$$\tilde{A}_f(f) = 0.391f + 36.3 \text{ [dB]}, \quad (14)$$

with f given in MHz.

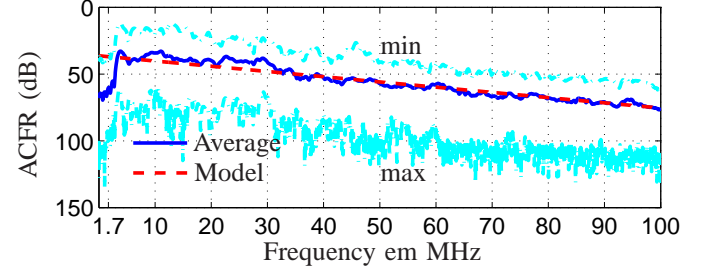


Fig. 6: Average channel frequency response of outdoor PLC channel measured in dB and its robust approach as a function of frequency.

C. Temporal dispersion

The RMS-DS statistics are indicated in Tab. II. As can be observed, the RMS-DS was smaller than 0.22 ms in 90% of the analyzed cases.

TABLE II: Root mean squared delay spread statistics of outdoor PLC channel in milliseconds.

	Min	Max	Mean	Std	90% above	90% below
RMS-DS	0.13	0.30	0.19	0.30	0.16	0.22

Fig. 7 shows the empirical cumulative distribution function (CDF) of the RMS-DS. The RMS-DS presented values between 129.7 μ s and 301.6 μ s following, with good approximation, the inverse gaussian probability distribution ($\mu = 0.186993$, $\lambda = 8.71957$).

D. Root Mean Squared Delay Spread versus Average Channel Attenuation

The relation between ACA and RMS-DS in outdoor PLC channel can be observed in Fig. 8. This relation can be modeled by robust linear approach based on the mean square error criterion, given by

$$\sigma_\tau = -0.01 \times 10^{-2} A_f + 0.19 \text{ [\mu s]}, \quad (15)$$

where σ_τ is the RMS-DS in microseconds.

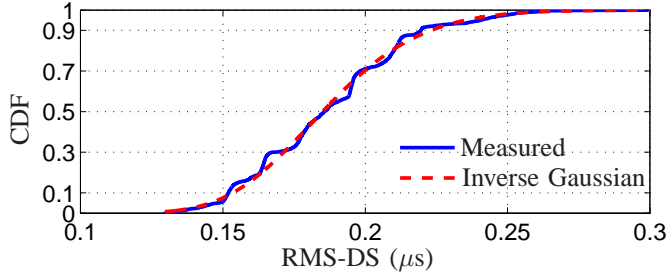


Fig. 7: Cumulative distribution function of root-mean-square delay spread of the outdoor PLC channel and the approaches by inverse gaussian distribution.

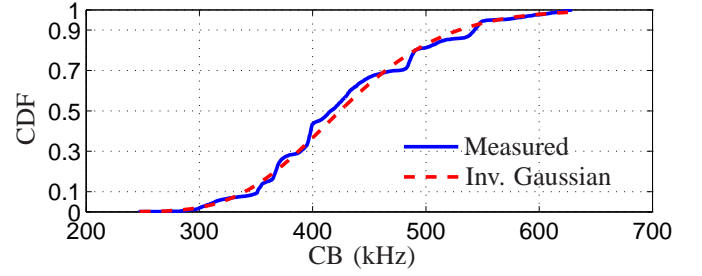


Fig. 9: Cumulative distribution function of coherence bandwidth of the outdoor PLC channel and the approaches by inverse gaussian and normal distribution.

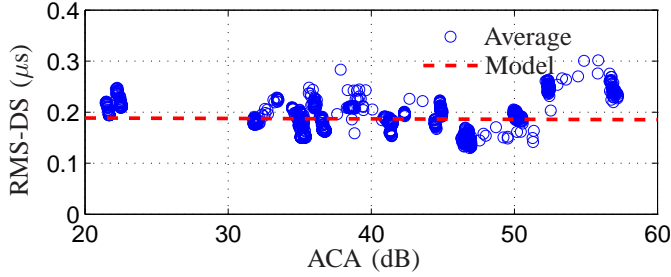


Fig. 8: Variation of RMS-DS due to ACA.

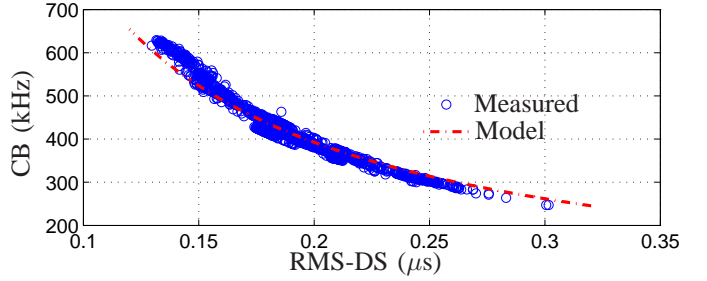


Fig. 10: RMS delay spread *versus* coherence bandwidth ($\varphi = 0.9$).

TABLE III: Coherence bandwidth statistics for $\gamma = 0.9$ of outdoor PLC channel in kHz.

	Min	Max	Mean	Std	90% above	90% below
CB	247.20	629.21	430.57	75.00	351.24	542.74

E. Coherence Bandwidth

The CB statistics are indicated in Tab. III, where it is observed that in 90% of the analyzed cases CB is higher than 351.24 kHz.

The empirical CDF of CB is shown in Fig. 9, when $\gamma = 0.9$ is considered. In this case, CB varies from 247.2 kHz up to 629.2 kHz following, with good approximation, a inverse Gaussian probability distribution ($\mu = 430.57$, $\lambda = 14,323.9$).

F. Root Mean Squared Delay Spread versus Coherence Bandwidth

The relationship between RMS-DS and CB can be verified in Fig. 10. The derived model was obtained through a robust approximation following a hyperbolic curve, which can be represented by

$$B_c^{0.9} = \frac{78.5}{\sigma_\tau}, \quad (16)$$

where $B_c^{0.9}$ refers to the CB when $\varphi = 0.9$ in kHz and σ_τ is the RMS-DS in μ s.

G. Coherence time

Fig. 11 illustrates the average evolution of the coherence index between analyzed Brazilian outdoor PLC channels. As can be seen, the occurrence of some valleys in the coherence index are due to abrupt change of the CIR that occurs in the passage through zero of the fundamental frequency of the electrical energy network.

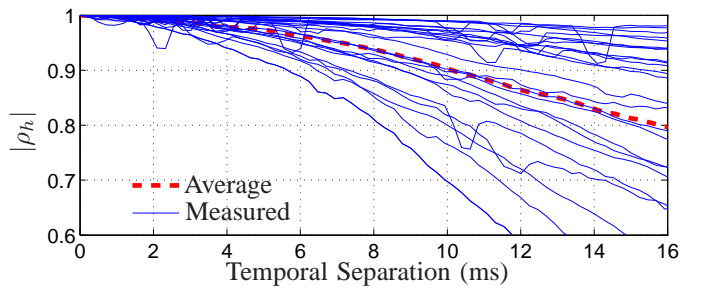


Fig. 11: Average evolution of the coherence index between outdoor PLC channels.

Fig. 12 depicts the cumulative distribution function of the PLC channel coherence time. As can be seen, only in 20% of the analyzed cases the coherence time was less than approximately 2 ms for $\beta = 0.99$, and 5 ms for $\beta = 0.95$.

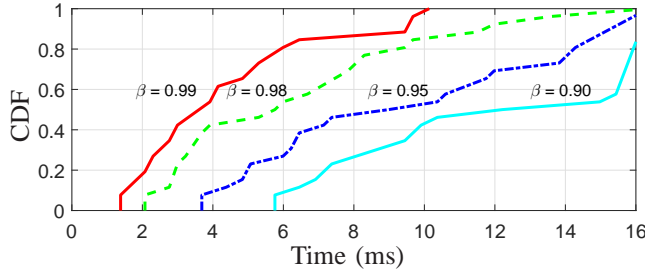


Fig. 12: Cumulative distribution function of coherence time of outdoor PLC channel.

The CT statistics are indicated in Tab. IV, considering $\beta = \{0.90; 0.95; 0.98; 0.99\}$. As can be observed, the coherence time observed from the measurement campaign was not lower than 1.38 ms and 5.76 ms, for $\beta = 0.99$ and $\beta = 0.90$, respectively. The highest CT value indicated in the TAB was limited by the storage capacity of the consecutive CFRs of the measurement equipment (723 CFRs) adopted in the measurement campaign.

TABLE IV: Coherence time statistics of outdoor PLC channel in ms.

β	Min	Max	Mean	Std	90% above	90% below
0.99	1.38	10.14	4.50	2.70	1.59	9.49
0.98	2.07	>16.36	6.55	3.83	2.49	11.70
0.95	3.69	>16.36	9.84	4.56	4.10	15.27
0.90	5.76	>16.36	12.28	4.21	6.18	16.36

H. Noise

In this work, each measured noise group has $N_v = 3,500,000$ samples and it is classified as background noise if all of its samples assume values less than V_{lim} . Otherwise, that is, the measured noise group has some sample with an amplitude greater than or equal to V_{lim} , it receives the classification of impulsive noise. Fig. 13 illustrates the two classes of noise adopted to model the noise of LV-PDN when $V_{lim} = 0.05$ V. In the Figure above the peak value of the noise amplitude did not exceed the decision threshold V_{lim} , so this group of N_v samples is classified as background noise. In the figure below, it is possible to identify that there are samples from the group where their amplitudes exceed the decision threshold, so the group is classified as impulsive noise.

Fig. 14 illustrates the PSD averaged of the two group of measured noise, background and impulsive noise, classified as described above.

The PSD of background and impulsive noise can be modeled by

$$S_n(f) = a + b \log_{10} |f| \quad \text{in dBV}^2/\text{Hz}, \quad (17)$$

where a and b are parameters dependent on the location of the measurements and f is the frequency in MHz. The values of a and b that model the noise present in the Brazilian LV-PDN

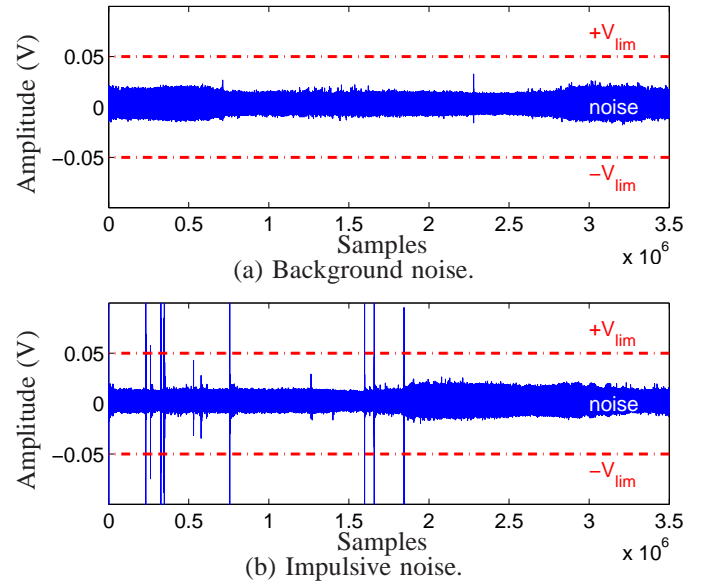


Fig. 13: Classification of the noise measured as a noise peak amplitude function (a) background noise and (b) impulsive noise.

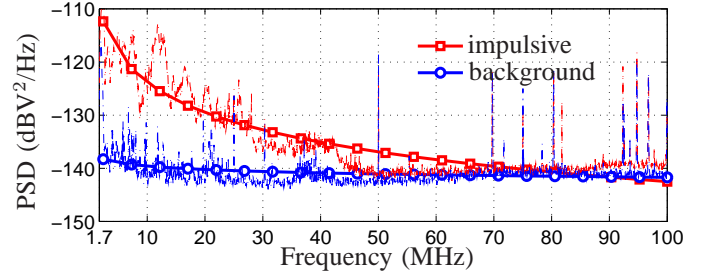


Fig. 14: Average PSD both background and impulsive noises of the low voltage electric power distribution networks and their respective models.

when considering the band of frequency of 1.7 MHz up to 100 MHz are indicated in Tab. V.

TABLE V: Parameters for noise models

Type of Noise	a	b
background	-137.5	-2.1
impulsive	-105.3	-18.6

I. Achievable data rate

Thus, we have ADR estimate of the outdoor PLC channel equivalent of a frequency selective channel whose restrictions on the transmitted signal and additive noise are those described in this section. It was adopted $|H[k]|^2 = 10^{-5}$, $k = 0, 1, \dots, N-1$, i.e., $\tilde{A}_f(50 \text{ MHz}) \approx 50 \text{ dB}$ (Fig. 6). Fig. 15

shows the achievable data rate of outdoor PLC in the presence both background and impulsive noise when considering the frequency band of 1.7-100 MHz.

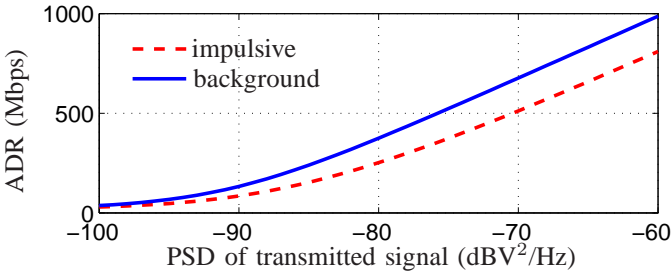


Fig. 15: Achievable data rate of the outdoor PLC channel in the presence both impulsive and background noise.

Finally, the main parameters that aid in the characterization of Brazilian outdoor PLC channel are summarized in Tab.VI.

V. CONCLUSION

This work presented the results of a comprehensive measurement campaign with the aim of characterizing and modeling the Brazilian LV-PDN as a means of data communication in the frequency band from 1.7 MHz up to 100 MHz.

Concerning the calculation of the coherence band and coherence time, it has been proposed to consider the outdoor PLC channel as having scattering uncorrelated and stationary in the broad sense. This modeling proved to be feasible since the lowest coherence time of the PLC outdoor channel found during the measurement campaign was 207 μ s, which is much longer than 23,4 μ s in which corresponds to the duration of the transmitted symbol.

Statistical models that represent the RMS-DS and CB of the measured channels were presented. Also, the temporal window statistic and average gain variation that occur due to periodic cyclic variations in the frequency response of the PLC channel was discussed at the first time.

Mathematical models, based on only two parameters, representing the background and impulsive noises present in LV-PDN have been proposed.

Finally, the achievable data rate of the outdoor PLC channel in the presence both impulsive and background noise was estimated.

ACKNOWLEDGMENT

The authors would like to thank, FINEP, FAPEMIG, CNPq, CAPES, P&D ANEEL, CEMIG, INERGE and Smarti9 for their financial supports.

REFERENCES

- [1] O. Andrisano, I. Bartolini, P. Bellavista, A. Boeri, L. Bononi, A. Borghetti, A. Brath, G. E. Corazza, A. Corradi, S. de Miranda, F. Fava, L. Foschini, G. Leoni, D. Longo, M. Milano, F. Napolitano, C. A. Nucci, G. Pasolini, M. Patella, T. S. Cinotti, D. Tarchi, F. Ubertini, and D. Vigo, "The need of multidisciplinary approaches and engineering tools for the development and implementation of the smart city paradigm," *Proceedings of the IEEE*, vol. 106, no. 4, pp. 738–760, April 2018.
- [2] D. Minoli, K. Sohraby, and B. Occhiogrosso, "Iot considerations, requirements, and architectures for smart buildings-energy optimization and next-generation building management systems," *IEEE Internet of Things Journal*, vol. 4, no. 1, pp. 269–283, Feb 2017.
- [3] M. Masera, E. F. Bompard, F. Profumo, and N. Hadjsaid, "Smart (electricity) grids for smart cities: Assessing roles and societal impacts," *Proceedings of the IEEE*, vol. 106, no. 4, pp. 613–625, April 2018.
- [4] L. Atzori, A. Iera, and G. Morabito, "The internet of things: A survey," *Computer Networks*, vol. 54, no. 15, pp. 2787 – 2805, 2010. [Online]. Available: <http://www.sciencedirect.com/science/article/pii/S1389128610001568>
- [5] Y. Mehmood, F. Ahmad, I. Yaqoob, A. Adnane, M. Imran, and S. Guizani, "Internet-of-things-based smart cities: Recent advances and challenges," *IEEE Communications Magazine*, vol. 55, no. 9, pp. 16–24, 2017.
- [6] L. d. M. B. A. Dib, V. Fernandes, M. de L. Filomeno, and M. V. Ribeiro, "Hybrid plc/wireless communication for smart grids and internet of things applications," *IEEE Internet of Things Journal*, vol. 5, no. 2, pp. 655–667, April 2018.
- [7] Y. Yan, Y. Qian, H. Sharif, and D. Tipper, "A survey on smart grid communication infrastructures: Motivations, requirements and challenges," *IEEE Communications Surveys Tutorials*, vol. 15, no. 1, pp. 5–20, Jan. 2013.
- [8] J. Han, J. D. Jeong, I. Lee, and S. H. Kim, "Low-cost monitoring of photovoltaic systems at panel level in residential homes based on power line communication," *IEEE Transactions on Consumer Electronics*, vol. 63, no. 4, pp. 435–441, November 2017.
- [9] G. Artale, A. Cataliotti, V. Cosentino, D. D. Cara, R. Fiorelli, S. Guadiana, N. Panzavacchia, and G. TinÀ, "A new low cost power line communication solution for smart grid monitoring and management," *IEEE Instrumentation Measurement Magazine*, vol. 21, no. 2, pp. 29–33, April 2018.
- [10] T. Willie, "Broadband over power lines," in *IEEE ISPLC*, Mar. 2006, pp. 1–1.
- [11] T. R. Oliveira, A. A. Picorone, S. L. Netto, and M. V. Ribeiro, "Characterization of brazilian in-home power line channels for data communication," *Electric Power Systems Research*, vol. 150, pp. 188 – 197, 2017. [Online]. Available: <http://www.sciencedirect.com/science/article/pii/S0378779617302006>
- [12] F. Corripio, J. Arrabal, L. del Rio, and J. Munoz, "Analysis of the cyclic short-term variation of indoor power line channels," *IEEE J. Sel. Areas Commun.*, vol. 24, no. 7, pp. 1327–1338, Jul. 2006.
- [13] A. Musolino, M. Raugi, and M. Tucci, "Cyclic short-time varying channel estimation in OFDM power-line communication," *IEEE Trans. Power Del.*, vol. 23, no. 1, pp. 157–163, Jan. 2008.
- [14] M. Zimmermann and K. Dostert, "An analysis of the broadband noise scenario in power-line networks," in *IEEE ISPLC*, 2000.
- [15] —, "A multipath model for the powerline channel," *IEEE Trans. Commun.*, vol. 50, no. 4, pp. 553–559, 2002.
- [16] M. Tlich, A. Zeddami, F. Moulin, and F. Gauthier, "Indoor power-line communications channel characterization up to 100 MHz ; part i: One-parameter deterministic model," *IEEE Trans. Power Del.*, vol. 23, no. 3, pp. 1392 –1401, Jul. 2008.
- [17] —, "Indoor power-line communications channel characterization up to 100 MHz; part ii: Time-frequency analysis," *IEEE Trans. Power Del.*, vol. 23, no. 3, pp. 1402 –1409, Jul. 2008.
- [18] A. Tonello, F. Versolatto, and A. Pittolo, "In-home power line communication channel: Statistical characterization," *IEEE Transactions on Communications*, vol. 62, no. 6, pp. 2096–2106, Jun. 2014.
- [19] W. Liu, H.-P. Widmer, J. Aldis, and T. Kaltenschnee, "Nature of power line medium and design aspects for broadband plc system," in *International Zurich Seminar on Broadband Communications*, 2000, pp. 185–189.
- [20] T. Prasad, S. Srikanth, C. Krishnan, and P. Ramakrishna, "Wideband

TABLE VI: Brazilian outdoor PLC channel statistics

Parameters	Min	Max	Mean	Std	90% above	90% below	Distribution
T_{W120} [ms]	0.73	0.98	1.40	0.12	0.73	1.15	
ACA [dB/m]			0.40				
ACFR [dB/MHz]			0.40				
RMS-DS [μ s]	0.13	0.30	0.19	0.03	0.16	0.22	Inv. Gaussian
CB ^{*1} [kHz]	247.2	629.2	430.6	75.01	351.24	542.74	Inv. Gaussian
CT ^{*2} [ms]	2.07	>16.3	6.55	3.83	2.49	11.70	

Note 1: $\gamma = 0.9$ Note 2: $\beta = 0.98$

characterization of low voltage outdoor powerline communication channels in india,” in *ISPLC*, 2001.

- [21] L. G. da Silva Costa, A. C. M. de Queiroz, B. Adebisi, V. L. R. da Costa, and M. V. Ribeiro, “Coupling for power line communications: A survey,” *Journal of Communication and Information Systems*, vol. 32, no. 1, 2017.
- [22] T. R. Oliveira, C. A. G. Marques, W. A. Finamore, S. L. Netto, and M. V. Ribeiro, “A methodology for estimating frequency responses of electric power grids,” *Journal of Control, Automation and Electrical Systems*, (online published), 2014.
- [23] J. Parsons, D. Demery, and A. Turkmani, “Sounding techniques for wideband mobile radio channels: A review,” *IEEE Proceedings in Communications, Speech and Vision*, vol. 138, no. 5, pp. 437–446, Oct. 1991.
- [24] M. V. Ribeiro, G. R. Colen, F. V. P. de Campos, Z. Quan, and H. V. Poor, “Clustered-orthogonal frequency division multiplexing for power line communication: When is it beneficial?” *IET Communications*, vol. 8, no. 13, pp. 2336–2347, Sept. 2014.
- [25] T. R. Oliveira, W. A. Finamore, and M. V. Ribeiro, “A sounding method based on OFDM modulation for PLC channel measurement,” in *Proc. IEEE International Symposium on Power Line Communications and Its Applications*, Mar. 2013, pp. 185–190.
- [26] F. Andrade, C. Marques, T. Oliveira, F. Campos, E. de Oliveira, and M. Ribeiro, “Preliminary analysis of additive noise on outdoor and low voltage electric power grid in Brazil,” in *IEEE International Symposium on Power Line Communications and Its Applications*, 2013, pp. 109–113.
- [27] A. A. M. Picorone, R. Sampaio-Neto, and M. V. Ribeiro, “Coherence time and sparsity of brazilian outdoor plc channels: A preliminary analysis,” in *IEEE International Symposium on Power Line Communications and its Applications*, Mar. 2014, pp. 1–5.
- [28] T. M. Cover and J. A. Thomas, *Elements of Information Theory*. John Wiley & Sons, 2006.